Article

Theoretical Investigation of the Deactivation of Ni Supported Catalysts for the Catalytic Deoxygenation of Palm Oil for Green Diesel Production

Sanaa Hafeez [1], **Sultan M Al-Salem** [2], **Kyriakos N Papageridis** [3], **Nikolaos D Charisiou** [3], **Maria A Goula** [3], **George Manos** [4,*] and **Achilleas Constantinou** [1,5]

1   Division of Chemical & Energy Engineering, School of Engineering, London South Bank University, London SE1 0AA, UK; hafeezs3@lsbu.ac.uk (S.H.); axilleas.constantinou@gmail.com (A.C.)
2   Environment & Life Sciences Research Centre, Kuwait Institute for Scientific Research, P.O. Box 24885, Safat 13109, Kuwait; ssalem@kisr.edu.kw
3   Laboratory of Alternative Fuels and Environmental Catalysis (LAFEC), Department of Chemical Engineering, University of Western Macedonia, GR-50100 Kozani, Greece; kpapageridis@gmail.com (K.N.P.); ncharisiou@uowm.gr (N.D.C.); mgoula@uowm.com (M.A.G.)
4   Department of Chemical Engineering, University College London, London WCIE 7JE, UK
5   Department of Chemical Engineering, Cyprus University of Technology, 57 Corner of Athinon and Anexartisias, Limassol 3036, Cyprus
*   Correspondence: g.manos@ucl.ac.uk

Publisher's Note: MDPI stays neutral with regard to jurisdictional claims in published maps and institutional affiliations.

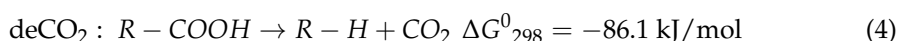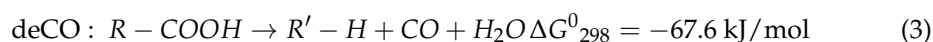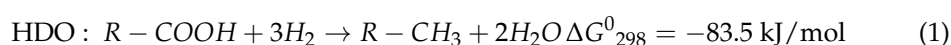**Abstract:** For the first time, a fully comprehensive heterogeneous computational fluid dynamic (CFD) model has been developed to predict the selective catalytic deoxygenation of palm oil to produce green diesel over an Ni/ZrO$_2$ catalyst. The modelling results were compared to experimental data, and a very good validation was obtained. It was found that for the Ni/ZrO$_2$ catalyst, the paraffin conversion increased with temperature, reaching a maximum value (>95%) at 300 °C. However, temperatures greater than 300 °C resulted in a loss of conversion due to the fact of catalyst deactivation. In addition, at longer times, the model predicted that the catalyst activity would decline faster at temperatures higher than 250 °C. The CFD model was able to predict this deactivation by relating the catalytic activity with the reaction temperature.

Keywords: green diesel; catalyst deactivation; selective deoxygenation; computational fluid dynamics (CFD)

1. Introduction

Green diesel as an environmentally friendly fuel has attracted considerable attention in recent years due to the fact of its high cetane number and high oxidative stability. Green diesel is a non-oxygenated hydrocarbon fuel produced from plant-derived oils. It can be used as a transportation fuel because its physiochemical properties are like those of diesel [1]. More recently, the conversion of non-edible sources into liquid hydrocarbons via hydrodeoxygenation (HDO) and deoxygenation (DO) has received considerable attention [2]. The deoxygenation of palm oil to produce green diesel can be summarised by an initial hydrogenation process, subsequently followed by DO reactions that can be classified as reactions of HDO, decarbonylation (deCO) and decarboxylation (deCO$_2$) [3] as shown below:

$$\text{HDO}: \ R-COOH + 3H_2 \rightarrow R-CH_3 + 2H_2O \ \Delta G^0_{298} = -83.5 \text{ kJ/mol} \tag{1}$$

$$\text{deCO}: \ R-COOH + H_2 \rightarrow R-H + CO + H_2O \ \Delta G^0_{298} = -17 \text{ kJ/mol} \tag{2}$$

$$\text{deCO}: \ R-COOH \rightarrow R'-H + CO + H_2O \ \Delta G^0_{298} = -67.6 \text{ kJ/mol} \tag{3}$$

$$\text{deCO}_2: \ R-COOH \rightarrow R-H + CO_2 \ \Delta G^0_{298} = -86.1 \text{ kJ/mol} \tag{4}$$

where R is a saturated alkyl group and R' is an unsaturated alkyl group.

Heterogeneous catalysts are cheaper, less corrosive, environmentally friendly and are easily regenerated, recovered and reused [4]. Nickel-supported catalysts have attracted great attention in recent years for green diesel production [2,3,5–16]. Catalyst deactivation is a troublesome issue when investigating the hydroprocessing of triglycerides. The mild acidity of the catalysts promotes the generation of many side reactions, as a result, coking of the catalyst may occur. Further reasons for the loss of catalytic activity may be sintering, poisoning or active metal leaching which reduces the number of active sites [17].

Kubička and Horáček [18] investigated the reasons for deactivation of hydrodesulphurization (HDS) catalysts during the deoxygenation of vegetable oils. The catalyst used in the study was sulphided $CoMo/\gamma$-Al_2O_3. The studies were performed in a fixed-bed reactor, and the reaction conditions were a hydrogen pressure of 3.5 MPa, temperature of 310 °C and a weight hourly space velocity (WHSV) of 2 h^{-1}. The results showed that the accumulation of alkalis encouraged the deactivation of the catalyst by causing the poisoning of the active sites. Furthermore, removing sulphur from the catalyst was found to negatively affect the deoxygenation reaction of the triglycerides. In addition, the loss of activity could be partly reversed by incorporating dimethyl disulfide to the feed. Nonetheless, the continuous addition of dimethyl disulfide was found to substantially lower the loss in catalytic activity.

Wang et al. [19] performed a catalyst deactivation study using a CoMoS catalyst. The feedstock used for the hydroprocessing reactions was waste cooking oil. It was found that the saturated hydrocarbons were predominantly generated on the MoS_2 active site found on the presulphided CoMoS catalyst. The unsaturated hydrocarbons were generated over the MoO_3 active sites on the used catalyst. The main reasons for the loss in catalytic activity were coke formation, loss of sulphur and the water side product. The deactivation caused by the loss of sulphur and water production was found to be partially reversible via in situ drying as well as resulphiding the used catalyst. The formation of coke could be reduced by using lower operating temperatures.

Gopinath et al. [20] studied the production of green diesel from the esterification of oleic acid and transesterification of jatropha oil using methanol. The catalysts developed in this work were sulphated Zr-KIT-6 mesoporous catalysts. The catalysts were synthesised using the one-step hydrothermal method using $SiO_2/P123/Bu$-$OH/HCl/H_2O$ gel as the acidic medium. The results showed that the optimum catalytic conversions, observed with the sulphated Zr-KIT-6 (20) catalyst, were 96% and 85% for the esterification and transesterification of oleic acid and jatropha oil, respectively. The reaction conditions employed to achieve these optimum conversions were a reaction temperature of 120 °C, 4 wt.% catalyst loading and a 20:1 methanol—oil ratio. The esterification yields acquired from oleic acid and jatropha oil were 95% and 80%, respectively. In addition, the spent catalysts could be recycled up to three cycles with significant activity and stability.

Wang et al. [21] investigated green diesel synthesis from the hydroprocessing of vegetable oil. The performance of several catalysts was compared, and it was found that the Mo_2C/AC catalysts had the superior performance with a 100% overall conversion and a cracking ratio of 21.01%. The lowest performing catalyst was observed to be the MoO/AC catalyst with an overall conversion of 56.05% and a cracking ratio of 18.55%. Furthermore, a study of optimisation was performed, and it was found that the optimum reaction conditions required to achieve the highest conversion for the Mo_2C/AC was a reaction temperature of 370 °C, hydrogen pressure of 3 MPa and an oil-solvent ratio of 20/60. Nonetheless, with each catalytic run, the conversion was found to decrease to 71.06%. Following catalyst regeneration, the conversion observed was 99.36%.

Gamal et al. [22] performed the deoxygenation of palm fatty acid distillate (PFAD) using a CoMo/AC catalyst. It was found that using equal ratios of Co and Mo in the CoMo/AC catalyst demonstrated the most superior efficiency for the deoxygenation pathway, which achieved a 92% and 89% yield of C8–C20 and n-(C15 + C17) hydrocarbons, respectively. The results showed that the CoMo/AC catalyst favoured the deoxygenation

route as opposed to CoMo catalysts supported on TiO_2 and Al_2O_3 that favoured the decarbonylation route. This is because the CoMo/AC catalyst has super acid base properties. Moreover, the catalyst could be reused for up to six cycles with a high selectivity of 78% and a hydrocarbon yield of 80–90%.

Vázquez-Garrido et al. [23] researched the effects of adding manganese to an Al_2O_3 support for producing NiMo catalysts for the hydroprocessing of soybean oil for green diesel production. The varying Mn contents of 1 and 5 mol% Mn were applied, whilst Al_2O_3–Mn_x (x = 1 or 5% mol Mn) were found by the sol-gel method. The results showed that the superior behaviour of the NiMo/Al_2O_3 catalyst was mainly due to the stable behaviour of the MnO on the aluminium support. This aids the redispersion of the Ni-promoted MoS_2 active phase. Additionally, there is a promising outlook to synthesise highly active NiMo catalysts, based on the addition of Mn, for the deoxygenation of vegetable oil feedstocks for the production of green diesel.

The current work aimed to investigate the deactivation of the Ni/ZrO_2 catalyst using computational modelling techniques for the first time. Detailed information regarding the catalytic performance of Ni/ZrO_2 can be sought in Papageridis et al. [3]. Theoretical modelling using CFD has proven to be a valuable tool for investigating many reactions generating renewable fuels [24–29]. A detailed heterogeneous CFD model has been developed to validate experimental data, and a good agreement was observed, proving the validity and robustness of the CFD model. The activity of the catalyst was correlated with the reaction temperature to demonstrate the deactivation of the catalyst at higher temperatures. Further parametric studies of reaction time and concentration were performed to assess the effect of the catalyst deactivation.

2. Results and Discussion

In order to assess the validity of the CFD model, a comparison with the experimental data was performed. Figure 1 depicts the comparison between the modelling and experimental data using the Ni/ZrO_2 catalyst. It can be observed that there was a very good agreement between the two sets of data, hence, confirming the high accuracy and robustness of the CFD models. The results show that the conversion of palm oil increased up to a maximum value of approximately 96%; however, it decreased significantly at temperatures greater than 300 °C for the Ni/ZrO_2 catalyst at t = 60 min. The experimental findings revealed that the Ni/ZrO_2 catalyst suffers from fast deactivation during the first hour of the reaction. After this period of fast deactivation, it was observed that the conversion of the triglycerides remained relatively stable for 4 h, with a further, much slower deactivation of up to 20 h [3]. Both the CFD and experimental results have demonstrated that the fast deactivation becomes more prominent at temperatures above 300 °C.
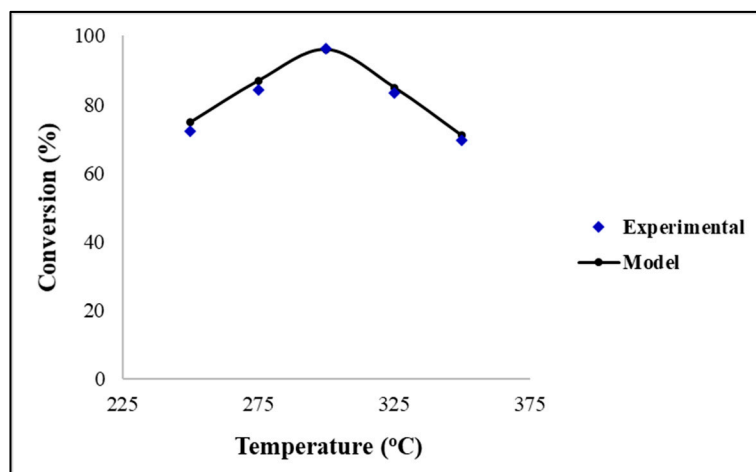
Figure 1. Conversion of TG against reaction temperature with Ni/ZrO_2. Reaction conditions: pressure = 30 bar, H_2/oil ratio = 1000 and inlet liquid flow = 0.1 mL/min.

Figure 2 displays the contribution of the HDO and deCO$_x$ reactions in the temperature range of 250–350 °C. It can be observed that the maximum yield of products obtained, via both the HDO and deCO$_x$ reactions, is at a reaction temperature of 300 °C. Moreover, both pathways show that the yields increase with temperatures up to 300 °C and then subsequently decrease due to the fact of catalyst deactivation. This is consistent with the findings depicted in Figure 1. The CFD model has proved a very good validation with the experimental data and can be utilised for further parametric studies.
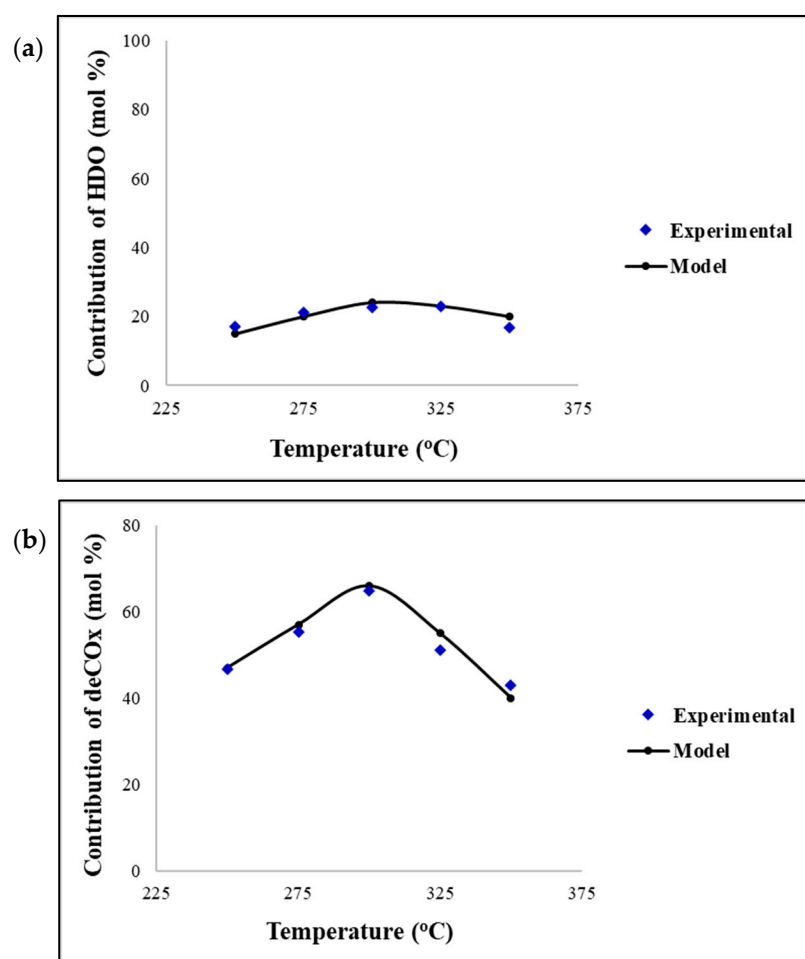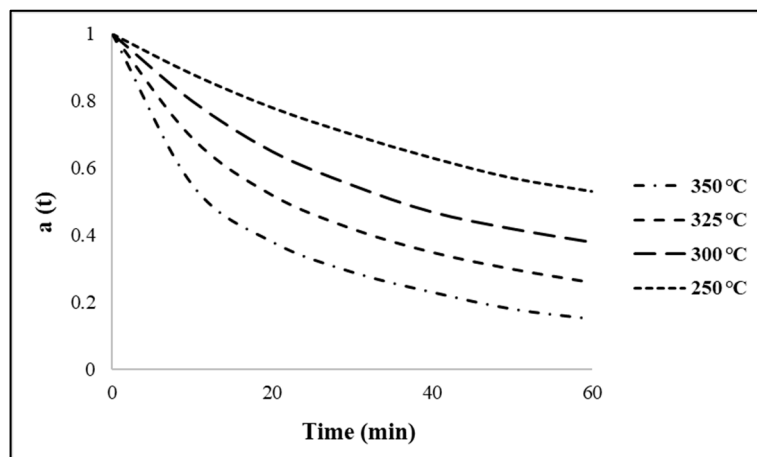

Figure 2. Contribution of the (**a**) HDO reactions and (**b**) deCO$_x$ reactions against reaction temperature. Reaction conditions: pressure = 30 bar, H$_2$/oil ratio = 1000 and inlet liquid flow = 0.1 mL/min.

Similar results were reported by Peng et al. [30] studying the deoxygenation of microalgae oil using a Ni/ZrO$_2$ catalyst. The experiments were performed in a trickle bed reactor, temperature 270 °C and a H$_2$ pressure of 40 bar. It was observed that n-C17 hydrocarbons were the major liquid product, with a maximum value of 68%, while total liquid alkanes were equal to 76%. Furthermore, Srifa et al. [31] investigated the catalytic HDO of palm oil over a NiMoS$_2$/γ-Al$_2$O$_3$ catalyst. It was found that temperatures lower than 300 °C resulted in a liquid product that was composed primarily of palmitic acid, stearic acid and slight trace quantities of triglycerides. In addition, increasing the temperature from 270 to 300 °C caused an increase of 26.7% to 89.8% in C15–C18 hydrocarbons production. However, an increase in temperature from 330 to 420 °C resulted in the reduction of the C15–C18 hydrocarbons from 88.9% to 37.9%. These results are consistent with those reported in the current theoretical work.

The relative activities of the catalyst with reaction time, at different temperatures, are plotted in Figure 3 for the Ni/ZrO$_2$ catalyst. The reaction temperature ranged from

250–350 °C. It is evidently observed that the catalytic activity decreased significantly with increasing temperature. Coking is one of the main reasons for catalyst deactivation in the HDO of triglycerides and is the result of carbonaceous (coke) material being deposited on the surface of the catalyst. This results in reduced hydrocarbon yields, catalytic activity, selectivity and life cycle time by covering the active sites on the catalysts and blocking the catalyst pores. The amount of coking typically increases with increasing temperature [32].

Figure 3. Activity parameter a(t) as a function of time at varying reaction temperatures with catalyst = Ni/ZrO$_2$. Reaction conditions: pressure = 30 bar, H$_2$/oil ratio = 1000 and inlet liquid flow = 0.1 mL/min.

Cordero-Lanzac et al. [33] studied catalyst deactivation during the HDO of triglycerides. The deactivation pathways of catalysts based on Pt–Pd supported on mildly acidic supports were assessed. It was found that using the Pt–Pd catalyst (supported on activated carbon) achieved higher HDO conversions, when compared to the conversions obtained using an equilibrated FCC catalyst as the support. The higher conversions obtained with the former catalyst resulted in a liquid product which consisted of mainly water. Nonetheless, the conditions of fast deactivation during the process favoured the production of solid and gas deposits as opposed to the liquid hydrocarbons, which possess the desirable properties to be used as a fuel. Furthermore, the conditions which promoted the production of coke further revealed the two main carbonaceous species that caused the deactivation. The unstable phenols found in the feedstock resulted in the accumulation of thermal lignin on the mesopores and external surface area of the catalyst at 400 °C. The thermal lignin is a deactivating species and has a high oxygen content. This deactivating species caused a substantial loss in catalytic activity, which can subsequently lead to blocking of the reactor due to the accumulation of these solids. At greater temperatures of approximately 450 °C, the phenols were observed to deoxygenate at a higher rate to produce aromatic species. As a result, there was a decrease in the rate of production of thermal lignin's; however, there was an increase in the production of the aromatic coke due to the condensation. The latter deactivating species had a larger aromatic content and a lower oxygen content. It was found that the fast deactivation could be prevented by implementing a pseudo steady-state conversion, which is imperative for the hydroprocessing reaction over longer time periods. By suppressing the formation of the alkyl phenols, the deactivation of the catalyst by coking can be reduced.

Li et al. [34] explored the deactivation of zeolite catalysts for the HDO of bio-oil derived from the pyrolysis of rice husk. The results showed that the loss in activity of the zeolite catalyst during the HDO reaction was mainly due to the fact of three stages. The first stage represents the rapid covering of the Lewis acid sites in the catalyst support by the oxygenated hydrocarbons; as a result, carbocations are produced which are precursors of soluble coke on the surface of the catalyst. This is subsequently followed by the stacking

of the soluble coke to produce chaotic filament-like carbon stands. Finally, these strands form into graphite carbon.

Another reason attributed to the loss of catalytic activity, for the deoxygenation of triglycerides, is sintering. This is due to the loss of active surface area arising from the prolonged exposure to high gas-phase temperatures. Taromi and Kaliaguine [35] investigated the HDO of triglycerides over Ni/γ-alumina catalysts for green diesel production. The results showed that at longer reaction times of 300–450 min, a loss of catalytic activity was observed, and the liquid conversion decreased significantly. This was subsequently followed by the conversion stabilising at a reaction time of 600 min. The authors related this fast deactivation to the adsorption of the unsaturated triglycerides on the surface of the catalyst (coke formation) or due to the sintering of the Ni species on the γ-alumina surface. Similar conclusions were also drawn by Papageridis et al. [36].

Figure 4 displays the reaction rate with the relative catalytic activity as a function of time. It can be observed that the rate of reaction was proportional to the reaction temperature with the fresh catalyst. However, as the reaction progressed through time (t = 60 min), the relative activity declined faster for temperatures greater than 300 °C. Subsequently, a maximum conversion was obtained at 300 °C and declined at higher temperatures due to the deactivation of the Ni/ZrO$_2$ catalyst (Figure 4a). This profile can be observed in Figure 1 and is consistent with the experimental findings. Nonetheless, if the initial strong deactivation were to continue at longer times (Figure 4b), the relative activity at 300 °C would decline stronger than the activity of 250 °C. As a result, the conversion of triglycerides would decrease with increasing temperatures.

Camargo et al. [37] studied the synthesis of green diesel by deoxygenation of oleic acid over Ni$_2$P-supported catalysts. The catalytic experiments were performed in an autoclave batch reactor at varying temperatures from 260 to 300 °C with an H$_2$ pressure of 50 bar. The results demonstrated that as the temperature increased from 260–280 °C, the number of C10–C18 hydrocarbons also increased. Nonetheless, there was a decrease from 280 to 300 °C. In addition, the yield of lighter hydrocarbons (C10–C16) increased with temperature, because cracking reactions were favoured at greater temperatures, and the production of C17 hydrocarbons peaked at 280 °C. The oleic acid conversion also depicted a maximum hydrocarbon production at 260–280 °C; however, it decreased from 280–300 °C for all catalysts. This phenomenon was attributed to catalyst deactivation, due to the coke deposition. These findings are consistent with those obtained in the CFD modelling study.

Salam et al. [38] investigated the effect of phosphorous (P) as a poison in the formation of phospholipids during the HDO of oleic acid over a NiMo/γ-Al$_2$O$_3$ catalyst. The main products generated using the fresh sulphided catalyst were mainly C17–C18 alkanes, implying a promotion of the deoxygenation reactions. The catalyst characterisation study revealed that the generated species, aluminium phosphate, significantly affected the active phase dispersion by blocking the active sites, resulting in the blockage of the catalyst pores. In addition, there was a correlation between the formation of coke and the phospholipids observed in the feed.

Figure 5 displays the reaction rate with the relative activity as a function of temperature. It can be observed that the rate of reaction for the fresh catalyst (t = 0 min) increased as the temperature increased. This was expected, according to the Arrhenius law, prior to the catalyst exhibiting any loss of activity. At shorter times (t = 60 min), a maximum rate of reaction can be observed at 300 °C, indicating a loss of catalytic activity due to the coking or sintering at greater temperatures. Furthermore, at longer times (t = 110 min), the relative activity will decline at 300 °C, producing a profile which shows that the reaction rate decreases as the temperature increases. Figure 6 depicts the concentration time profile after a period of t = 60 min, for the Ni/ZrO$_2$ catalyst. It can be observed, the concentration of triglycerides decreased at all temperatures, but the greatest decrease was observed for 300 °C. This is consistent with the findings that state the maximum conversion was obtained at 300 °C. The decline in concentration was slower for 350 °C, due to the strong

effects of the catalyst deactivation, and for 250 °C due to the low reaction temperature catalysing the reaction.
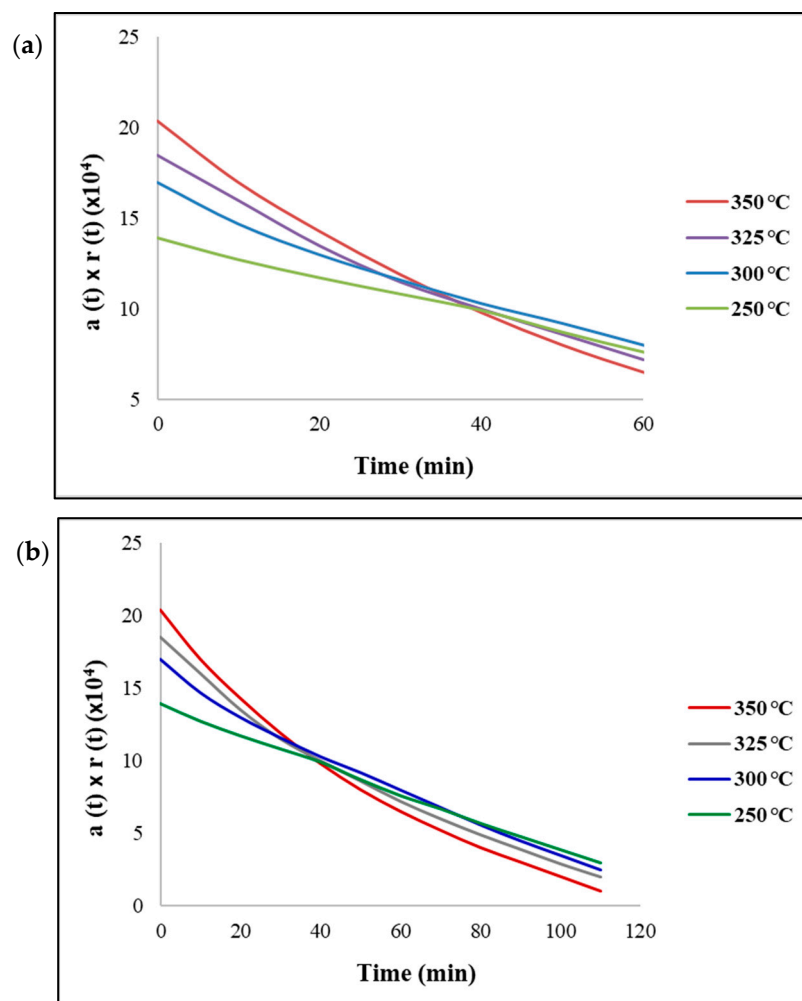
Figure 4. Reaction rate as a function of time with catalyst = Ni/ZrO$_2$ at (**a**) t = 60 min and (**b**) t = 120 min. Reaction conditions: pressure = 30 bar, H$_2$/oil ratio = 1000 and inlet liquid flow = 0.1 mL/min.
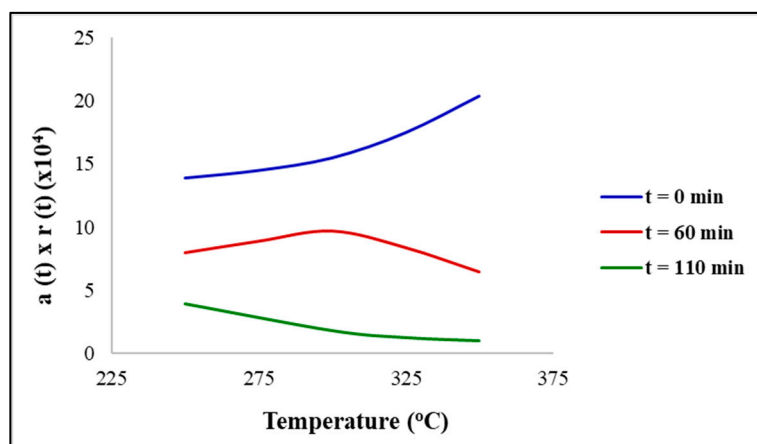
Figure 5. Reaction rate as a function of reaction temperature at varying times with catalyst = Ni/ZrO$_2$. Reaction conditions: pressure = 30 bar, H$_2$/oil ratio = 1000 and inlet liquid flow = 0.1 mL/min.
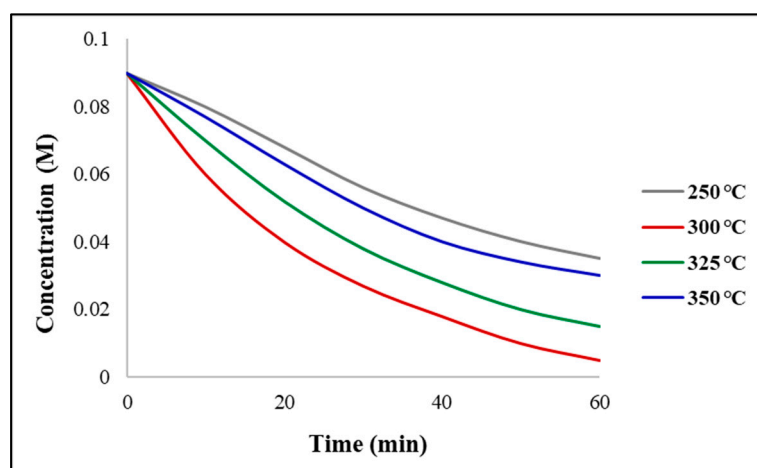
Figure 6. Inlet concentration time plots at varying temperatures with catalyst = Ni/ZrO$_2$. Reaction conditions: pressure = 30 bar, H$_2$/oil ratio = 1000, inlet liquid flow = 0.1 mL/min and t = 60 min.

Papageridis et al. [3] investigated the effect of operating parameters on the catalytic deoxygenation of palm oil for green diesel synthesis. The catalysts used were Ni supported on Al$_2$O$_3$, ZrO$_2$ and SiO$_2$ catalysts in a continuous flow fixed-bed reactor. The range of temperatures selected for the study were 250–400 °C. It was found that increasing the H$_2$ pressure caused an increase in paraffin conversion; however, increasing the temperature was only advantageous up to a maximum point for each catalyst. For the Ni/ZrO$_2$ catalyst, the conversion of the triglycerides was approximately 72% at 250 °C, and a maximum conversion of 96% was observed at 300 °C. Increasing the temperature above this maximum point led to a significant decrease in conversion of approximately 62% at 375 °C. The temperatures at which the maximum conversion was achieved for the other catalysts were 375 °C and 350 °C for the Ni/Al$_2$O$_3$ and Ni/SiO$_2$ catalysts, respectively.

3. Materials and Methods

3.1. Experimental Procedure

The selective catalytic deoxygenation of palm oil experiments took place in a Autoclave Engineers BTRS-Jr (Erie, PA, USA) stainless-steel continuous flow tubular packed-bed reactor (length 30 cm, internal diameter 0.7 cm) with a total volume of 12 mL. The liquid flow rate of the feed was set to 0.2 mL/min. The experiments were performed in the temperature range of 250–400 °C, a hydrogen pressure of 30 bar, an H$_2$/oil ratio of 1000 and a liquid hourly space velocity (LHSV) of 1.2–4.8 h^{-1}. Further details of the experimental setup of which the CFD modelling was based upon can be found in [3].

3.2. CFD Modelling Methodology

The CFD models provided a valuable tool to investigate the particle-fluid transport behaviour. Performing experimental studies to investigate the production of green diesel can often be costly as well as time consuming. On the other hand, conducting CFD studies can deliver well detailed information on the space–time phenomena regarding reaction conditions (temperature, pressure, concentrations and flow) inside the reactor whilst avoiding issues which may arise with experimental work. Hence, a CFD is a desirable approach to perform parametric studies and facilitates the comprehensive study of the physiochemical processes involved.

A 2D packed-bed reactor was modelled under the assumptions that mass, temperature and velocity profiles occur in the radial and axial directions only. Further assumptions were as follows: (1) unsteady-state and laminar flow applies in the reactor; (2) application of ideal gas behaviour for components in the gas phase; (3) the axial fluid velocity is continuous with constant physical properties and transport coefficients. The solid spherical catalyst

particles used were Ni supported on ZrO_2. Figure 7 shows a schematic representation of the reactor that the CFD model was based upon.
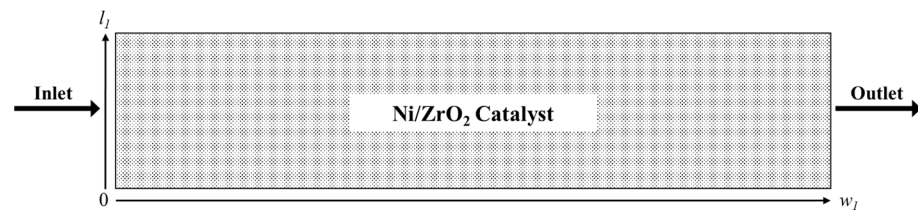
Figure 7. Schematic representation of the packed bed reactor used for the CFD modelling simulation.

Various studies have proposed kinetic models for Ni-supported catalysts. The kinetic model used to represent the catalytic deoxygenation of palm oil was based on an alumina-supported nickel catalyst (15NiAl) [39]. The reactions were assumed to be first order with respect to the components in the liquid phase and partial pressure of H_2 in the gas phase. The continuity equation integrated the diffusion and convection for the reacting fluids in the packed-bed reactor and is described as:

$$\frac{\partial c_i}{\partial t} + \nabla \times J_i S_b + u \times \nabla c_i = R \tag{5}$$

where c_i is the concentration of the reacting fluids (mol/m^3), R is the reaction rate expression for the species (mol/(m^3·s)), u is the velocity (m/s), and J_i is the molar flux diffusive vector (mol/(m^2·s)), and S_b is the active specific surface area (m). The multiphase chemical reaction, which occurs within the catalyst particles, was incorporated with the conservation equations using the Reactive Pellet Bed feature in COMSOL® version 5.3 (Stockholm, Sweden). The mass balance around a spherical shell at r_{dim} and a predetermined 1D extra dimension on the normalised radius of the catalyst pellet particle ($r = r_{dim}/r_{pe}$) is displayed as:

$$4\pi N \left\{ r^2 r_{pe}{}^2 \varepsilon_{pe} \frac{\partial c_{pe,i}}{\partial t} + \nabla \times \left(-r^2 D_{i,eff} \nabla c_{pe,i} \right) = r^2 r_{pe}{}^2 R_{pe} \right\} \tag{6}$$

where N is the number of pellets per unit volume of the packed bed, $D_{i,eff}$ is the effective diffusion coefficient of the reacting fluid inside the pores of the catalyst pellet and R_{pe} is the reaction rate term in mol/(m^3·s) per unit volume of pellet.

The hydrodynamics of the reactor are represented by the Navier–Stokes equation. The continuity equations validating the conservation of mass and momentum are expressed as:

$$\frac{\partial \rho}{\partial t} + \nabla \times (\rho u) = 0 \tag{7}$$

$$\rho \frac{\partial u}{\partial t} + \rho (u \times \nabla) u = \nabla \times [-PI + \tau] + F \tag{8}$$

where P is pressure (Pa), τ is the viscous stress tensor (Pa) and F is the volume force vector (N/m^3).

The experimental findings showed that the conversion of triglycerides decreases with temperature; this can be explained by catalyst deactivation due to the fact of coke deposition (coking) or sintering. In order to predict this trend using CFD modelling, the activity of the catalyst must be obtained relative to the reaction temperature. The activity of the catalyst, a, decreased exponentially with increasing temperature, and can be given as:

$$a = e^{\frac{-k_d}{t}} \tag{9}$$

where k_d is the deactivation rate constant and can be expressed as:

$$k_d = A e^{\left(-\frac{E_d}{RT} \right)} \tag{10}$$

where A is the pre-exponential factor, E_d is the deactivation energy (kJ/mol), R is the universal gas constant (J/(mol $\times$ K)) and T is the temperature (K) [40].

The modelling assumptions combined with the appropriate mass balances and governing boundary conditions were computed using COMSOL Multiphysics® software version 5.3. The boundary conditions of the continuous flow reactor are represented by:

$$\text{at } x = 0; \ c_i = c_{i,in}, \ u_y = 0, \ u_x = u_{in}, \ \frac{\delta^2 P}{\delta x^2} = 0 \tag{11}$$

$$\text{at } x = w_1; \ \frac{\delta c_i}{\delta x} = 0, \ u_y = 0, \ \frac{\delta u_x}{\delta x} = 0, \ P = P_{out} \tag{12}$$

$$\text{at } y = 0; \ c_i = 0, \ u_r = 0, \ \frac{\delta u_x}{\delta y} = 0, \ \frac{\delta P}{\delta y} = 0 \tag{13}$$

$$\text{at } r = 1; \ c_{i,p} = c_{i,ps} \tag{14}$$

$$\text{at } r = 0; \ \frac{\delta c_{i,p}}{\delta r} = 0 \tag{15}$$

4. Conclusions

A CFD model was successfully developed to investigate the synthesis of green diesel from palm oil over a Ni/ZrO$_2$ catalyst. A sound validation was acquired between the modelling and experimental results, confirming the validity of the CFD model. The deactivation of the catalyst was successfully correlated with the reaction temperature, and it was reported that coking or sintering were often the greatest reasons for loss in activity at elevated temperatures. In the case for both catalysts, the conversion of palm oil improved with temperatures up to a maximum of 300 °C. Any subsequent increase in temperature led to a decrease in conversion. Nonetheless, at longer periods of this fast deactivation, the model predicted that the catalyst activity decreased with temperatures greater than 250 °C.

The developed CFD model was applicable to any catalytic reaction system which had a deactivation rate temperature dependence that followed the Arrhenius equation. The CFD model explains the unusual phenomenon of the conversion not monotonically increasing with temperature. This is because the deactivation rate increases with temperature; at higher temperatures, the deactivation is stronger causing the reaction to slow down and the conversion to decrease. The comprehensive CFD model developed in this study demonstrated a very good validation for the selective deoxygenation of palm oil using an Ni/ZrO$_2$ catalyst. As a result, the model offers a promising outlook to be used as a basis for other reaction systems demonstrating the production of green diesel by altering the feedstock and the type of catalyst. Theoretical modelling tools are a valuable method to assess the validity of experimental results, as well as performing parameter optimisation studies to enhance the green diesel production process.

Utilising CFD is beneficial, as comprehensive information regarding space–time variations in fluid component flows, temperatures and concentrations can be obtained in an effortless manner as opposed to experimental work, which can often be time consuming and costly. Hence, CFD is a promising approach/methodology in calculating the parameters facilitating a thorough study of the physicochemical processes involved and the design of experimental studies. Future work could be directed towards minimising catalyst deactivation to enhance the green diesel production process.

Author Contributions: Conceptualization, G.M. and A.C.; Formal analysis, S.H. and S.MA.-S.; Investigation, S.H., K.NP. and N.DC.; Methodology, S.MA.-S., G.M. and A.C.; Software, S.H.; Supervision, N.DC., M.A.G., G.M. and A.C.; Writing—original draft, S.H.; Writing—review & editing, S.H., SM.A.-S., M.AG., G.M. and A.C. All authors have read and agreed to the published version of the manuscript.

References

1. Hafeez, S.; Al-Salem, S.; Constantinou, A. Membrane Reactors for Renewable Fuel Production and Their Environmental Benefits. In *Membranes for Environmental Applications*; Springer: Cham, Switzerland, 2020; pp. 383–411.

2. Kamaruzaman, M.F.; Taufiq-Yap, Y.H.; Derawi, D. Green diesel production from palm fatty acid distillate over SBA-15-supported nickel, cobalt, and nickel/cobalt catalysts. *Biomass Bioenergy* **2020**, *134*, 105476. [CrossRef]

3. Papageridis, K.; Charisiou, N.D.; Douvartzides, S.L.; Sebastian, V.; Hinder, S.J.; Baker, M.A.; AlKhoori, S.; Polychronopoulou, K.; Goula, M.A. Effect of operating parameters on the selective catalytic deoxygenation of palm oil to produce renewable diesel over Ni supported on Al_2O_3, ZrO_2 and SiO_2 catalysts. *Fuel Process. Technol.* **2020**, *209*, 106547. [CrossRef]

4. Saba, T.; Estephane, J.; El Khoury, B.; El Khoury, M.; Khazma, M.; El Zakhem, H.; Aouad, S. Biodiesel production from refined sunflower vegetable oil over KOH/ZSM5 catalysts. *Renew. Energy* **2016**, *90*, 301–306. [CrossRef]

5. Aliana-Nasharuddin, N.; Asikin-Mijan, N.; Abdulkareem-Alsultan, G.; Saiman, M.I.; Alharthi, F.A.; Alghamdi, A.A.; Taufiq-Yap, Y. Production of green diesel from catalytic deoxygenation of chicken fat oil over a series binary metal oxide-supported MWCNTs. *RSC Adv.* **2020**, *10*, 626–642. [CrossRef]

6. Ameen, M.; Azizan, M.T.; Ramli, A.; Yusup, S.; Abdullah, B. The effect of metal loading over Ni/γ-Al_2O_3 and Mo/γ-Al_2O_3 catalysts on reaction routes of hydrodeoxygenation of rubber seed oil for green diesel production. *Catal. Today* **2019**, *355*, 51–64. [CrossRef]

7. Choo, M.-Y.; Oi, L.E.; Ling, T.C.; Ng, E.-P.; Lin, Y.-C.; Centi, G.; Juan, J.C. Deoxygenation of triolein to green diesel in the H2-free condition: Effect of transition metal oxide supported on zeolite Y. *J. Anal. Appl. Pyrolysis* **2020**, *147*, 104797. [CrossRef]

8. Gousi, M.; Kordouli, E.; Bourikas, K.; Symianakis, E.; Ladas, S.; Kordulis, C.; Lycourghiotis, A. Green Diesel Production over Nickel-Alumina Nanostructured Catalysts Promoted by Copper. *Energies* **2020**, *13*, 3707. [CrossRef]

9. Hachemi, I.; Kumar, N.; Mäki-Arvela, P.; Roine, J.; Peurla, M.; Hemming, J.; Salonen, J.; Murzin, D.Y. Sulfur-free Ni catalyst for production of green diesel by hydrodeoxygenation. *J. Catal.* **2017**, *347*, 205–221. [CrossRef]

10. Hongloi, N.; Prapainainar, P.; Seubsai, A.; Sudsakorn, K.; Prapainainar, C. Nickel catalyst with different supports for green diesel production. *Energy* **2019**, *182*, 306–320. [CrossRef]

11. Kordouli, E.; Pawelec, B.; Bourikas, K.; Kordulis, C.; Fierro, J.L.G.; Lycourghiotis, A. Mo promoted Ni-Al_2O_3 co-precipitated catalysts for green diesel production. *Appl. Catal. B Environ.* **2018**, *229*, 139–154. [CrossRef]

12. Liu, P.; Chen, C.; Zhou, M.; Xu, J.; Xia, H.; Shang, S.; Jiang, J. Metal–organic framework-derived Ni-based catalyst for the hydrotreatment of triolein into green diesel. *Sustain. Energy Fuels* **2021**, *5*, 1809–1820. [CrossRef]

13. Liu, Y.; Sotelo-Boyás, R.; Murata, K.; Minowa, T.; Sakanishi, K. Hydrotreatment of jatropha oil to produce green diesel over trifunctional Ni–Mo/SiO_2–Al_2O_3 catalyst. *Chem. Lett.* **2009**, *38*, 552–553. [CrossRef]

14. Nikolopoulos, I.; Kogkos, G.; Kordouli, E.; Bourikas, K.; Kordulis, C.; Lycourghiotis, A. Waste cooking oil transformation into third generation green diesel catalyzed by nickel–alumina catalysts. *Mol. Catal.* **2020**, *482*, 110697. [CrossRef]

15. Papadopoulos, C.; Kordouli, E.; Sygellou, L.; Bourikas, K.; Kordulis, C.; Lycourghiotis, A. W promoted Ni-Al_2O_3 co-precipitated catalysts for green diesel production. *Fuel Process. Technol.* **2021**, *217*, 106820. [CrossRef]

16. Ruangudomsakul, M.; Osakoo, N.; Wittayakun, J.; Keawkumay, C.; Butburee, T.; Youngjan, S.; Faungnawakij, K.; Poo-arporn, Y.; Kidkhunthod, P.; Khemthong, P. Hydrodeoxygenation of palm oil to green diesel products on mixed-phase nickel phosphides. *Mol. Catal.* **2021**, 111422. [CrossRef]

17. Alvarez-Galvan, M.C.; Campos-Martin, J.M.; Fierro, J.L. Transition metal phosphides for the catalytic hydrodeoxygenation of waste oils into green diesel. *Catalyst* **2019**, *9*, 293. [CrossRef]

18. Kubička, D.; Horáček, J. Deactivation of HDS catalysts in deoxygenation of vegetable oils. *App. Catal. A Gen.* **2011**, *394*, 9–17. [CrossRef]

19. Wang, H.; Li, G.; Rogers, K.; Lin, H.; Zheng, Y.; Ng, S. Hydrotreating of waste cooking oil over supported CoMoS catalyst–Catalyst deactivation mechanism study. *Mol. Catal.* **2017**, *443*, 228–240. [CrossRef]

20. Gopinath, S.; Kumar, P.S.M.; Arafath, K.Y.; Thiruvengadaravi, K.; Sivanesan, S.; Baskaralingam, P. Efficient mesoporous SO_4^{2-}/Zr-KIT-6 solid acid catalyst for green diesel production from esterification of oleic acid. *Fuel* **2017**, *203*, 488–500. [CrossRef]

21. Wang, F.; Xu, J.; Jiang, J.; Liu, P.; Li, F.; Ye, J.; Zhou, M. Hydrotreatment of vegetable oil for green diesel over activated carbon supported molybdenum carbide catalyst. *Fuel* **2018**, *216*, 738–746. [CrossRef]

22. Gamal, M.S.; Asikin-Mijan, N.; Khalit, W.N.A.W.; Arumugam, M.; Izham, S.M.; Taufiq-Yap, Y. Effective catalytic deoxygenation of palm fatty acid distillate for green diesel production under hydrogen-free atmosphere over bimetallic catalyst CoMo supported on activated carbon. *Fuel Process. Technol.* **2020**, *208*, 106519. [CrossRef]

23. Vázquez-Garrido, I.; López-Benítez, A.; Guevara-Lara, A.; Berhault, G. Synthesis of NiMo catalysts supported on Mn-Al_2O_3 for obtaining green diesel from waste soybean oil. *Catal. Today* **2021**, *365*, 327–340. [CrossRef]

24. Gollakota, A.R.; Subramanyam, M.D.; Kishore, N.; Gu, S. CFD simulations on the effect of catalysts on the hydrodeoxygenation of bio-oil. *RSC Adv.* **2015**, *5*, 41855–41866. [CrossRef]

25. Hafeez, S.; Aristodemou, E.; Manos, G.; Al-Salem, S.; Constantinou, A. Computational fluid dynamics (CFD) and reaction modelling study of bio-oil catalytic hydrodeoxygenation in microreactors. *React. Chem. Eng.* **2020**, *5*, 1083–1092. [CrossRef]
26. Hafeez, S.; Aristodemou, E.; Manos, G.; Al-Salem, S.; Constantinou, A. Modelling of packed bed and coated wall microreactors for methanol steam reforming for hydrogen production. *RSC Adv.* **2020**, *10*, 41680–41692. [CrossRef]
27. Hafeez, S.; Sanchez, F.; Al-Salem, S.M.; Villa, A.; Manos, G.; Dimitratos, N.; Constantinou, A. Decomposition of Additive-Free Formic Acid Using a Pd/C Catalyst in Flow: Experimental and CFD Modelling Studies. *Catalyst* **2021**, *11*, 341. [CrossRef]
28. Subramanyam, M.D.; Gollakota, A.R.; Kishore, N. CFD simulations of catalytic hydrodeoxygenation of bio-oil using Pt/Al$_2$O$_3$ in a fixed bed reactor. *RSC Adv.* **2015**, *5*, 90354–90366. [CrossRef]
29. Fortunate, O.; Kishore, N. Computational Fluid Dynamics Investigation on Catalytic Hydrodeoxygenation of a Bio-Oil Model Compound in a Fluidized Bed Reactor. *J. Therm. Sci. Eng. App.* **2021**, *13*, 061018. [CrossRef]
30. Peng, B.; Yuan, X.; Zhao, C.; Lercher, J.A. Stabilizing catalytic pathways via redundancy: Selective reduction of microalgae oil to alkanes. *J. Am. Chem. Soc.* **2012**, *134*, 9400–9405. [CrossRef]
31. Srifa, A.; Faungnawakij, K.; Itthibenchapong, V.; Viriya-Empikul, N.; Charinpanitkul, T.; Assabumrungrat, S. Production of bio-hydrogenated diesel by catalytic hydrotreating of palm oil over NiMoS$_2$/γ-Al$_2$O$_3$ catalyst. *Bioresour. Technol.* **2014**, *158*, 81–90. [CrossRef]
32. Cheng, S.; Wei, L.; Zhao, X.; Julson, J. Application, deactivation, and regeneration of heterogeneous catalysts in bio-oil upgrading. *Catalyst* **2016**, *6*, 195. [CrossRef]
33. Cordero-Lanzac, T.; Palos, R.; Hita, I.; Arandes, J.M.; Rodriguez-Mirasol, J.; Cordero, T.; Bilbao, J.; Castano, P. Revealing the pathways of catalyst deactivation by coke during the hydrodeoxygenation of raw bio-oil. *Appl. Catal. B Environ.* **2018**, *239*, 513–524. [CrossRef]
34. Li, Y.; Zhang, C.; Liu, Y.; Tang, S.; Chen, G.; Zhang, R.; Tang, X. Coke formation on the surface of Ni/HZSM-5 and Ni-Cu/HZSM-5 catalysts during bio-oil hydrodeoxygenation. *Fuel* **2017**, *189*, 23–31. [CrossRef]
35. Taromi, A.A.; Kaliaguine, S. Hydrodeoxygenation of triglycerides over reduced mesostructured Ni/γ-alumina catalysts prepared via one-pot sol-gel route for green diesel production. *App. Catal. A Gen.* **2018**, *558*, 140–149. [CrossRef]
36. Papageridis, K.N.; Charisiou, N.D.; Douvartzides, S.; Sebastian, V.; Hinder, S.J.; Baker, M.A.; AlKhoori, A.A.; AlKhoori, S.I.; Polychronopoulou, K.; Goula, M.A. Continuous selective deoxygenation of palm oil for renewable diesel production over Ni catalysts supported on Al$_2$O$_3$ and La$_2$O$_3$–Al$_2$O$_3$. *RSC Adv.* **2021**, *11*, 8569–8584. [CrossRef]
37. de Oliveira Camargo, M.; Pimenta, J.L.C.W.; de Oliveira Camargo, M.; Arroyo, P.A. Green diesel production by solvent-free deoxygenation of oleic acid over nickel phosphide bifunctional catalysts: Effect of the support. *Fuel* **2020**, *281*, 118719. [CrossRef]
38. Abdus Salam, M.; Creaser, D.; Arora, P.; Tamm, S.; Lind Grennfelt, E.; Olsson, L. Influence of bio-oil phospholipid on the hydrodeoxygenation activity of NiMoS/Al$_2$O$_3$ catalyst. *Catalysts* **2018**, *8*, 418. [CrossRef]
39. Yenumala, S.R.; Maity, S.K.; Shee, D. Reaction mechanism and kinetic modeling for the hydrodeoxygenation of triglycerides over alumina supported nickel catalyst. *React. Kinet. Mech. Catal.* **2017**, *120*, 109–128. [CrossRef]
40. Fogler, H. Chapter 10: Catalysis and Catalytic Reactors. *Elem. Chem. React. Eng.* **2016**, *5*, 454–456.